Periodic polarization duty cycle tunes performance and adhesion of anodic electroactive biofilms

Xu Zhang[1†], Amanda K. Luther[1], Korneel Rabaey[1,2], Antonin Prévoteau[1,2]*

Author Affiliations:

[1] Center for Microbial Ecology and Technology (CMET), Ghent University, Coupure Links 653, 9000 Ghent, Belgium

[2] Centre for Advanced Process Technology for Urban Resource Recovery (CAPTURE), 9000 Ghent, Belgium

[†] present address: Department of BioSciences, Rice University, Houston, TX 77005, USA

Corresponding Author

* Phone: 32(0)9 264 5973 ; e-mail: Antonin.Prevoteau@UGent.be.

Highlights

- Duty cycles of 50%, 67%, 80% and 91% were tested for impact on EAB growth
- EABs grown at 50% deliver best performances in the long term
- EABs periodically detach at 50%, followed by quick and more efficient regrowth
- Removal of aged EABs by 30s of H_2 evolution allows for regrowth of higher performing EABs
- Those insights could help optimizing microbial electrochemical systems

Keywords

Current production, anodic polarization, biofilm detachment, charge storage, aged biofilms, microbial fuel cells

Abstract

Periodic polarization can improve the performance of anodic electroactive biofilms (EABs). The impact of the half-period duration was previously investigated at constant duty cycle (50%), i.e., the proportion of a period during which the electrode is polarized. Here, we cultured eight EABs on glassy carbon electrodes at four different duty cycles (50%, 67%, 80% and 91%) by varying the time interval under open circuit conditions, while keeping the polarization duration at 10 s. The shorter duty cycles slightly slowed initial growth but produced EABs generating higher faradaic currents. The total charge recovery over 38 days increased with decreasing duty cycles from 0.53 kC.cm−2 (duty cycle of 91%) to 1.65 kC.cm−2 (50%). EABs with the shortest duty cycle fully detached twice from the electrode surface, but detachments were quickly followed by the formation of more efficient EABs. We then carried out controlled removal of some aged and low current-producing EABs by applying a 30s cathodic current (H2 evolution at −15 mA.cm−2) and observed the subsequent rapid development of fresh EABs displaying better electrochemical performance. Our results illustrate that well-chosen dynamic controls of electrode potentials can substantially improve the average current production of EABs, or allow a simple replacement of underperforming EABs.

Introduction

Electroactive microorganisms can exchange electrons with solid state electron donors and acceptors, such as polarized electrodes, metals, or oxides. Some can convert chemical energy into electrical energy by oxidizing a variety of organic compounds and delivering low potential

electrons to an electrode. Some of these "anodic" bacteria can form relatively thick conductive electroactive biofilms (EABs), the most studied being *Geobacter sulfurreducens* in single-species biofilm and enriched *Geobacter* species in multispecies biofilms. Extensive work has been devoted towards increasing the maximum current density of the microbial anode to enhance the power production of microbial fuel cells (MFCs) [1], the production rate of microbial electrocatalysis cells (MECs) [2], or the sensitivity of EAB-based biosensors [3]. Numerous studies have investigated the impact of electrode material and associated surface modifications to favor higher current densities in anodic EABs [4-7]. Others have genetically engineered electroactive microorganisms to better understand the role of redox proteins putatively associated with the electron transfer pathways or to maximize electron transfer rates [8-10]. Conversely, much less work has been devoted to the impact of the electric input ─ specifically the electrode potential and its temporal variations ─ on the development of EABs and on the current density they can generate.

Electroactive biofilms are typically grown under continuous polarization, i.e., at constant load for MFCs and constant potential in 3-electrode setups. Conversely, some MFCs have been studied under intermittent polarization (switching between closed and open-circuit conditions) to generate transient but higher power density compared to constantly connected MFCs (Table 1) [11-14].

Table 1. Literature review of studies performing periodic polarization in bioelectrochemical systems (BESs) using microbial anodes. Listed: the range of time intervals under open circuit (t_{OCP}), under anodic polarization (t_{pol}) and the corresponding optimal "duty cycle" reported ($t_{pol}/[t_{pol} + t_{OCP}]$).

BES	t_{OCP} / s	t_{pol} / s	Operation	Duty cycle-opt	Ref.
Microbial anodes in MFCs					
Mixed culture	5-100	1200	NA	NA	[11]
	1.8-60	$14\times t_{OCP}$	24 h	93.3%	[15]
	0.6-7	3	8~12 h	83 %	[12]
	0.0019-5	900-3600	24h	95 %	[16]
	30-3600	30-900	10 h	86%	[13]
	0.5-10	1-300	4 cycles	86%	[14]
	0.1 to 40	0.03~540	11 h	75 %	[17]
	600-1800	3600	2 cycles	67%	[18]
Microbial anodes in 3-electrode setup					
G. sulfurreducens	600-3600	5400s at 0.4 V	1 cycle	86%	[19]
G. sulfurreducens	30-600	30-600s at 0.3V	24 h	NA	[20]
Mixed culture	300-3600	600-7200s at −0.4V	15 cycles	67 %	[21]
Mixed culture	600-7200	600-10800s at −0.3V	1 cycle	67 %	[22]
Mixed culture	60	600-10800s at −0.3V	40 cycles	75 %	[23]
Mixed culture	1-300	1-300s at −0.1V	10 days	NA	[24]
Mixed culture	10	10s at −0.1V	35 days	NA	[25]
Mixed culture	5-300	5-300s at −0.35V	30 days	NA	[26]

When the circuit is disconnected, electrons generated by the microbial metabolism accumulate in the redox cofactors of the EAB, inducing a current spike when the circuit is reconnected [18-21]. The open circuit voltage (OCV) of the MFCs also increase during disconnection because the open circuit potential (OCP) of microbial anodes quickly decreases following the reduction of extracellular cytochromes close to the electrode surface [24, 27]. The increase of both current and initial operating voltage during reconnection leads to a transient but substantial power gain. When the ON/OFF period is adequately chosen, the energy generated by the MFC under periodic connection has been shown to be higher than when the device is constantly connected.

Intermittent energy harvesting mode of an MFC enhanced the maximum power generation by 111% when compared to a continuous harvesting mode.[28] Another MFC operating under periodic polarization delivered 33% more power output on average than under continuous polarization [17]. The fraction of a periodic signal during which the electrode is anodically polarized (duty cycle, D) could alter the performance of microbial electrodes. To the extent of our knowledge, optimal duty cycles have been proposed to be between 75% and 95% to maximize power production (Table 1) [16]. These studies generally assessed the impact of the duty cycle only in the short term (< 1 day for testing a single duty cycle) [12, 21, 22], and typically assume the biological system to be at steady-state when assessing the impact of the electrical signal, whereas the characteristics of a biofilm are slowly but dynamically evolving under the application of external stimuli over a longer time scale. Our previous studies have shown that non-continuous electric signals substantially modify the intrinsic properties of EABs within a few days [24, 25]. When applied during EAB formation, adequate periodic polarization can greatly increase the average concentration of charge carriers in EABs dominated by *Geobacter sp.* (10.6 mM of electron equivalent vs. 2.9 mM for continuously polarized EABs) [24]. Our observations indicated that the enhancement might be due to an overexpression of c-type cytochromes induced by the periodic limitation of electron acceptor, i.e., during the periods of open circuit. This increase in charge carrier concentration strongly correlated with increases in (i) maximum catalytic current density, (ii) charge storage capacity and (iii) ability to transport electrons over the biofilm thickness [24]. We also observed that it was possible to tune the properties of already mature biofilms by modifying the periodical signal, and that this change was reversible within a few days [25]. A specific periodic polarization input could even induce sporadic detachment of aged EABs from a smooth electrode surface while continuously polarized EABs remained steadily adhered [25]. Considering the dynamic impact of the applied electric signal on EABs, it appears relevant to assess how the duty cycle can tune EABs under longer term operation than previously reported studies.

Here, we first demonstrate the impact of different duty cycles on acetate-fed, anodic EABs grown under periodic polarization on glassy carbon electrodes. We determine the optimal duty cycle by periodically monitoring the apparent ‘steady-state’ catalytic current and the total amount of charge generated over time by the EABs. In a second phase, using the same EABs, we apply the optimal duty cycle to all EABs to assess if it could improve the electrochemical performance of mature EABs previously grown under less optimal duty cycles. We also discuss the relationship between the applied polarization signals and biofilm detachments. We finally

show that an aged, low performing biofilm can be quickly removed from a smooth electrode surface by applying a short (30 s) but substantial negative current (− 15 mA.cm^{-2}), and that subsequently a better performing EAB quickly develops. We then discuss the possible outlook of periodic polarization for practical applications using microbial electrochemical systems.

Materials and methods

Reactor setup

An 8-electrode, 2-compartment reactor was set up as previously described [24, 29]. The 8 working electrodes were glassy carbon plates with 4 cm^2 geometric surface area (HTW, Germany), successively polished with alumina slurries (0.3 μm, 0.1 μm and 0.05 μm diameter, Buehler, USA). They were placed symmetrically around the circular anodic compartment, such that their conductive surfaces were equidistantly facing the counter electrode compartment in the center of the electrochemical cell. The anolyte was 700 mL of anaerobic M9 medium (chemical composition in Table S1) with 24 mM acetate as electron donor. The medium has a pH of 7.5 and is highly buffered (64 mM phosphate) to limit acidification within the EABs. It was continuously mixed by a magnetic stirrer (~ 300 rpm). A stainless-steel mesh was folded cylindrically (15 cm long and 2 cm diameter) and placed in the cathodic compartment as counter electrode. The cathodic compartment was filled with 50 mL of anaerobic modified M9 medium devoid of acetate. The catholyte was replaced every two days to alleviate alkalinity build-up due to the cathodic reaction (H_2 evolution). A cation exchange membrane was used to separate the two compartments (12.5 cm^2, Ultrex CMI-7000). A common Ag/AgCl reference electrode (3 M KCl, ALS, Japan, + 0.208 V vs. standard hydrogen electrode at 28 °C) was placed in the anodic compartment for all potential measurements. Electrochemical control and analyses were performed with a potentiostat (BioLogic, France). Experiments were carried out in a temperature-controlled room without exposure to natural light, at ~ 28 °C.

Cultivation of EABs under different duty cycle

The anolyte was inoculated at t = 0 with 35 mL (5 vol%) of fresh anolyte from an operating acetate-fed microbial anode. The reactor was first operated in batch mode for 4 days to enable microbial colonization of the electrode surface, then switched to continuous mode with continuous feeding of M9 medium through the anodic compartment (hydraulic retention time of 10 h) using a peristaltic pump (Watson-Marlow 323S, UK). This allowed acetate concentration to be maintained at saturation level for the metabolism of anodic EABs grown on flat electrodes [24].

The experiment was performed in 3 successive phases (Figure 1 provides an illustrative scheme):

Phase I: the 8 working electrodes were initially separated in 4 duplicate groups with variable open circuit time intervals (t_{OCP} = 1 s, 2.5 s, 5 s and 10 s). All electrodes shared a fixed polarization time of 10 s (t_{pol}) at − 0.1 V vs. Ag/AgCl, a potential within the anodic plateau current of *Geobacter*-dominated EABs, therefore allowing electron release to the anode at the maximum rate possible [29].

The "duty cycle" (D) is here defined as the ratio between the polarization time interval (allowing heterogeneous electron transfer between EABs and electrodes) and the total period:

$$D = \frac{t_{pol}}{t_{pol}+t_{OCP}} \qquad (1)$$

The corresponding duty cycles are 91% (t_{OCP} = 1 s), 80% (t_{OCP} = 2.5 s), 67% (t_{OCP} = 5 s) and 50% (t_{OCP} = 10 s). EABs grown under specific conditions will be designated with their respective duty cycle as $EAB_{91\%}$, $EAB_{80\%}$, $EAB_{67\%}$, and $EAB_{50\%}$. We selected the amplitude of t_{pol} (10 s) and the range of t_{OCP} (1 — 10 s) because we previously observed that 1 s and 10 s were the two half-periods inducing the best current and charge recovery for EAB grown only under 50% duty cycles [24]. We tested a higher range of duty cycles (50 — 91%) because the literature has been suggesting that optimal duty cycles would be within the 75 — 95%), though most studies focused on short-term measurements.

In order to maximize the number of duty cycles tested, no additional control under continuous polarization was performed since those were done in our previous studies clearly proving the positive impact of periodic polarization [24, 25]. This phase lasted for 38 days and allowed assessment of which duty cycle induced the best electrochemical performances for the EABs i.e. highest j_{ss} and charge recovery (*vide infra*).

Phase II: after 38 days of growth under their respective duty cycle, the polarization signal of all EABs was switched to a duty cycle of 50% (the optimal duty cycle as established from *Phase I*) in order to assess if the best signal could improve the performance of mature EABs previously grown under less optimal signals. This phase lasted for 42 days.

Phase III: here we wanted to assess if the removal of aged EABs delivering relatively low current, could induce the growth of fresh biofilms with better electrochemical performance. To do so, we applied a negative current of – 15 $mA.cm^{-2}$ for 30 s on 4 of the 8 electrodes (both duplicates of $EAB_{91\%}$ and $EAB_{50\%}$; a representative chronopotentiometry is displayed in Fig.

S1). The generation of H_2 bubbles and the rise of pH at the interface between electrode and biofilm immediately led to a fast and smooth removal of the 4 EABs. Periodic polarization was then immediately restarted at a duty cycle of 50% for all electrodes. The small amount of H_2 generated (36 µmol i.e., 50 µM assuming a 100 % faradaic efficiency for H_2) did not significantly impact the current output of the remaining EABs (see Fig. S2) and was washed away with the effluent.

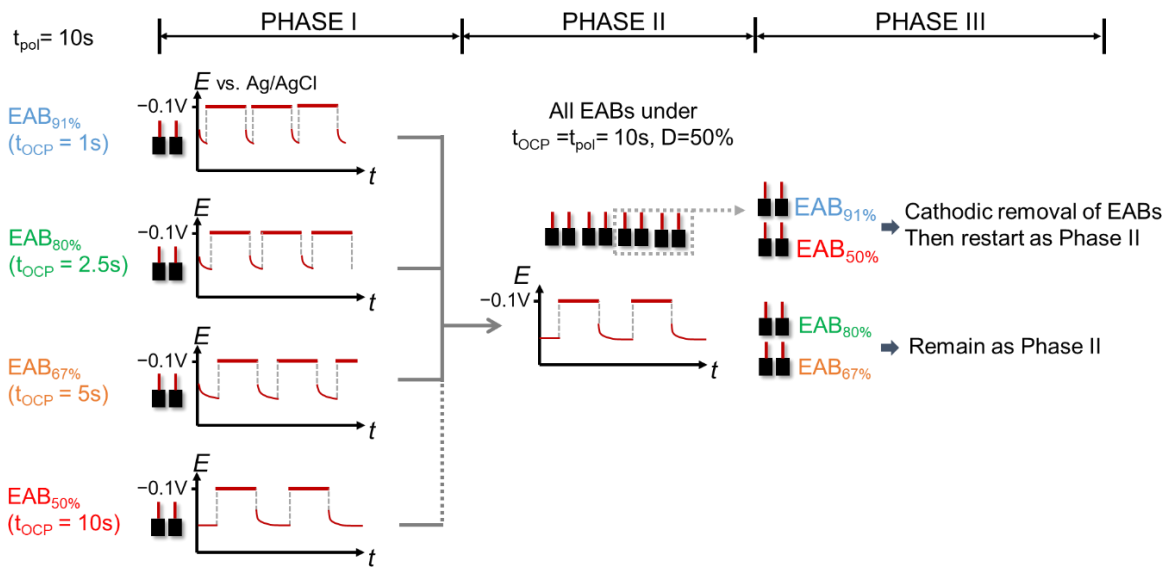

Figure 1. Schematic illustration of the different stages of the experiment. ***Phase I***: EABs are grown under different duty cycles (8 electrodes were separated into 4 duplicate groups with different OCP time intervals). ***Phase II***: all polarization signals are switched to a duty cycle of 50% (periods of 10 s of polarization followed by 10 s OCP). ***Phase III*****:** four EABs were removed by applying cathodic current from their underlying electrode before restarting the periodic polarization as in *phase II*.

Electrochemical analyses

The periodic discharge current does not reach an apparent steady-state at the end of the 10 s of polarization (Figure S3). Hence, for a fair comparison of electroactivity between EABs, we recorded a daily apparent 'steady-state' catalytic current density (j_{ss}) for each EAB after 1000 s of continuous polarization at – 0.1 V vs. Ag/AgCl. The respective periodic polarizations were immediately resumed at the end of j_{ss} recordings. The 1000 s measurement corresponds to only 1% of the periodic polarization applied every day and is not expected to have a substantial impact on the development and electroactivity of the EABs. This was confirmed by the identical profiles observed for the discharge currents recorded just before and just after the j_{ss} measurement (Figure S4).

We also define the gain of electric charge due to periodic polarisation when compared to continuous polarization ΔC (mC.cm^{-2}) per cycle, as:

$$\Delta C = Q_{1\,cycle} - Q_{ss} = \int^{1\,cycle} j.dt - j_{ss} \times 10 \qquad (2)$$

Where $Q_{1\,cycle}$ corresponds to the recorded charge transferred to the electrode during 1 period (i.e., 10 s of polarization) and Q_{ss} is the theoretical charge obtained during 10 s under the corresponding steady-state current recorded thereafter. ΔC therefore quantifies how the time-interval under OCP allows charging of the EABs with electrons that increase the subsequent discharge current when repolarized. We previously proved that for those EABs grown on flat electrodes, the extreme majority of the supplementary transient charge generated is of faradaic nature (pseudo-capacitive) and not resulting from the double-layer capacitance [24]. While ΔC allows comparison of the impact of the OCP on the discharge current, it does not allow comparison of the global charge production because of the difference in duty cycle tested.

To compare the evolution of global charge recovery over time, the amount of charge collected during 1 h (mC.cm^{-2}) of periodic polarization (therefore including the respective time under OCP) was obtained once a day by integration of the current density:

$$Q_{1h} = \int_{t}^{t+1h} j.dt \qquad (3)$$

Error bars on Figures represent 2-times the standard deviation of the mean (n = 2).

Results and Discussion

Phase I: growth, steady-state catalytic current (j_{ss}) and charge generation

Figure 2(A) shows the evolution of the apparent steady-state current density j_{ss} for the electrode under different duty cycles, starting from inoculation (t = 0). The current started to increase in a similar way for the EABs grown under the 3 higher duty cycles (67%, 80%, 91%), all reaching a 10 µA.cm^{-2} threshold after ~ 55 h. Conversely, the current increase for $EAB_{50\%}$ was slightly delayed, reaching 10 µA.cm^{-2} only after ~ 68h. This result shows that the shorter OCP time intervals (5 s, 2.5 s and 1 s) were short enough to not substantially impact the initial growth of $EAB_{67\%}$, $EAB_{80\%}$, and $EAB_{91\%}$, while the 10 s interval was sufficiently long to induce a considerable electron acceptor limitation and negatively impact the initial respiration rate and associated growth of the biofilms.

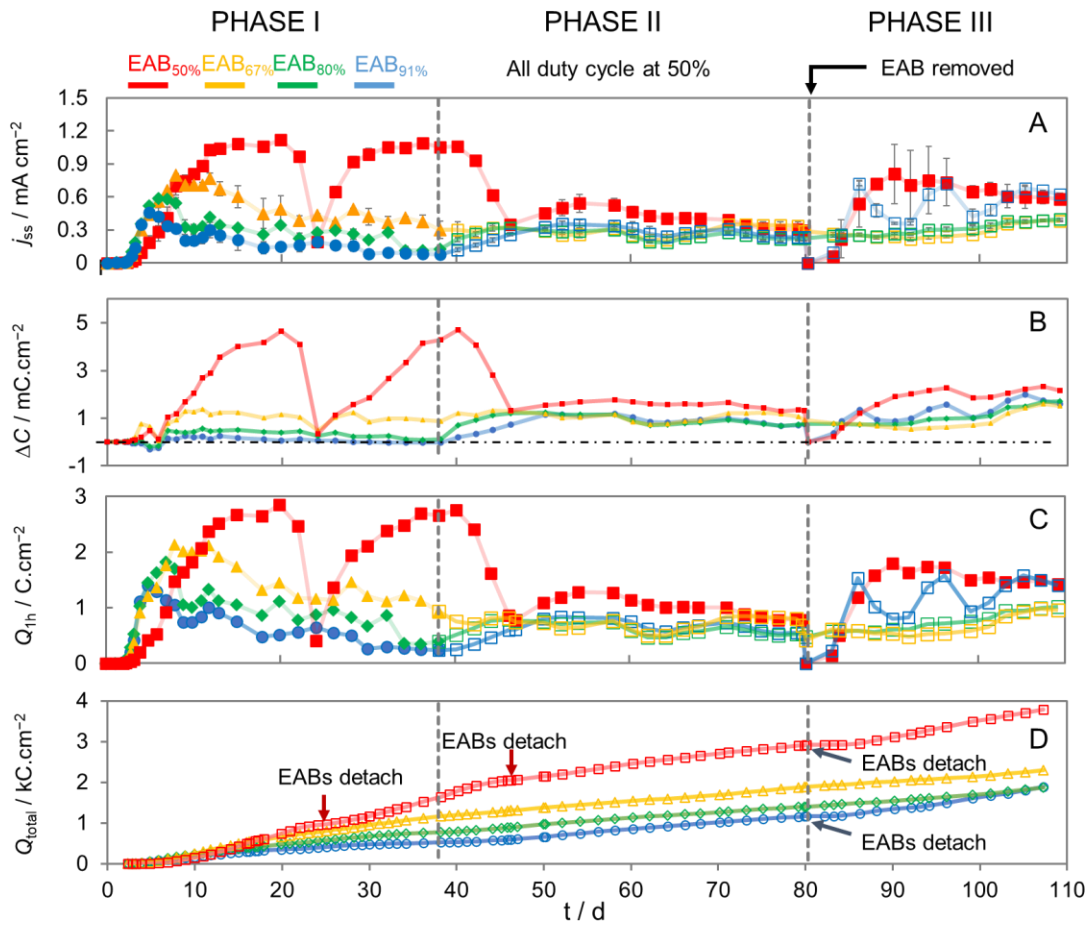

Figure 2. Evolution from inoculation for EABs grown at different duty cycle of: (A) apparent steady- state catalytic current; (B) electric charge gain induced by the periodic polarization; (C) electric charge collected per electrode over time intervals of 1 h (including the open circuit time intervals); (D) cumulative electric charge produced by EABs grown under different duty cycles.

The biofilms grown under higher duty cycles (above 50%) reached a local maximum in j_{ss} of 0.42 mA.cm^{-2} after 5 days ($EAB_{91\%}$), 0.58 mA.cm^{-2} after 6 days ($EAB_{80\%}$) and 0.8 mA.cm^{-2} after 8 days ($EAB_{67\%}$). The current then started to gradually decrease for these EABs, first substantially, then with only a slight negative drift almost stabilizing at the end of Phase I around 0.08 mA.cm^{-2} ($EAB_{91\%}$ and $EAB_{80\%}$) and 0.37 mA.cm^{-2} ($EAB_{67\%}$). The evolution of j_{ss} was different for $EAB_{50\%}$. At day 12, the current first reached a plateau at the highest current density (~ 1.1 mA.cm^{-2}) lasting for about 1 week. Similar to a previous observation [25], a dramatic current decrease occurred from day 20 to day 24 (from 1.1 mA.cm^{-2} to 0.2 mA.cm^{-2}) simultaneously for both $EAB_{50\%}$. This is attributed to the concomitantly observed detachment of a large proportion of both $EAB_{50\%}$ from their electrode surface. The decrease in current occurred steadily over the 4 days, without any occurrence of large punctual steps, illustrating the fact that the detachment was a continuous process. Images of the biofilm detachments are

provided in Figure 3. Afterwards, the current recovered to its value prior to detachment in about 4 days, at ~ 1 mA.cm^{-2} and remained stable through the end of Phase I.

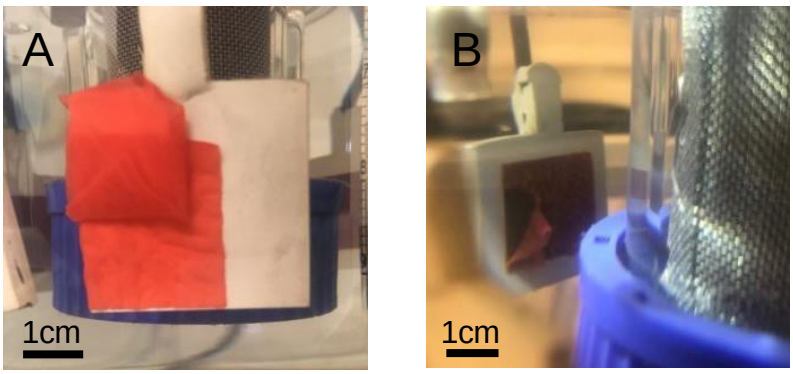

Figure 3. Pictures of spontaneous detachments for $EAB_{50\%}$. (A) First detachment at day 24: two EABs (red squares) had detached and adhered to the white insulating back side of an electrode. (B) Second detachment at day 46: detachment is initiating with part of the EAB peeling off from the left side of the electrode surface.

The evolution of the gain of charge ΔC is presented on Figure 2(B). As expected, the value decreased with increasing duty cycle i.e., decreasing the interval during which the EABs store electrons (OCP). It stays almost at zero for $EAB_{91\%}$, illustrating that the charge accumulation during OCP had little impact on the subsequent discharge current for such a high duty cycle and short OCP interval (1 s). The gain of charge per cycle stabilizes around 0.5 mC.cm^{-2} for $EAB_{80\%}$, 1 mC.cm^{-2} for $EAB_{67\%}$ and 4 mC.cm^{-2} for $EAB_{50\%}$. Interestingly, ΔC does not evolve exactly as j_{ss} along the duty cycle, illustrating that charge storage ability of EABs is not strictly correlated to their catalytic activity. Typically, ΔC remained almost constant from day 8 while j_{ss} notably decreased for $EAB_{80\%}$ and $EAB_{67\%}$, or ΔC still increased after day 12 while j_{ss} already stabilized for $EAB_{50\%}$. In other words, the ratio j_{ss}/ΔC decreased over time for maturing EABs that had already reached their peak in j_{ss} (Figure S5). This could be explained by the final phase of EAB growth before they reach their quasi-steady state in thickness. It has been shown that most of the catalytic activity of *G. Sulfurreducens* EAB is located along the first layers of biofilm located in close vicinity to the electrode surface (< 10 µm), where the highest concentration of extracellular redox cofactors are oxidized and available for accepting electrons generated during microbial metabolism [30]. This active layer is the one responsible for most of the j_{ss} amplitude. Nevertheless, those EABs typically grow until 40 to 80 µm thickness, where bacteria located further from the electrode generate very little continuous current yet are still able to store some electrons that could be released during repolarization steps, as previously shown by spectroelectrochemical techniques [31-33]. This decrease in the ratio of j_{ss}/ΔC is therefore likely linked to the growth of EABs beyond the active layers.

Overall, the results suggest two interesting implications:

i. Duty cycles above 67% (coupled with OCP time intervals below 5 s) are not producing EABs capable of conserving high electroactivity in the long term. The maximum j_{ss} and current stability decreased with increasing duty cycle. The reason is very likely that an OCP time interval that is too short does not induce sufficient electron acceptor limitation to enhance the EAB performance.

ii. Decreases in current after reaching a local maximum have been commonly reported for anodic EABs [4, 24, 34]. Here we observed that EAB detachment could be an operational strategy to recover higher current densities by growing new biofilms instead of keeping aged ones.

Whereas j_{ss} and ΔC provide information on the electroactivity and ability of the EABs to store and deliver charges under specific periodic polarization, the total amount of charge generated under intermittent operation is the most relevant parameter from an applied perspective, e.g., to recharge a battery to sustain environmental sensors [35]. The evolution of the charge generated during intervals of 1h of respective periodic polarization is presented in Figure 2(C).

The overall pattern for the evolution of Q_{1h} is relatively similar to the one recorded for j_{ss}, with $EAB_{50\%}$ producing the highest amount of charge, plateauing twice (before detachment and regeneration) around 2.7 $C.cm^{-2}$ for 1 h of intermittent operation. Other EABs produced lower Q_{1h} that decreased over time to stabilize at the end of Phase I. As with j_{ss} and ΔC, the stabilized values of Q_{1h} decreased with increasing duty cycle applied to the electrode: 1 $C.cm^{-2}$ ($EAB_{67\%}$) 0.6 $C.cm^{-2}$ ($EAB_{80\%}$) and 0.3 $C.cm^{-2}$ ($EAB_{91\%}$). Considering the variation of Q_{1h} throughout the experiment, the cumulative amount of charge collected over time (Q_{total}) is also available for the different EABs (Figure 2(D)). $EAB_{50\%}$ produced the highest amount of charge with 1.65 $kC.cm^{-2}$ during the 38 days of Phase I, followed by EABs of increasing duty cycle i.e., $EAB_{67\%}$ (1.16 $kC.cm^{-2}$), $EAB_{80\%}$ (0.78 $kC.cm^{-2}$), and $EAB_{91\%}$ (0.53 $kC.cm^{-2}$). Overall, these results illustrate that lower duty cycles induce the growth of more efficient EABs and generate more charge over time.

Phase II: switching to optimal periodic polarization and natural detachments of aged biofilm

After more than one month of growth, the current production of $EAB_{50\%}$ was still the highest at 1 $mA.cm^{-2}$, after having recovered from the first spontaneous detachment. We assessed the possibility to enhance the performance of mature EABs by applying the best duty cycle of 50% to all EABs (Figure 2, Phase II). This transition induced an increase in j_{ss} for $EAB_{91\%}$ and $EAB_{80\%}$ from 0.08 $mA.cm^{-2}$ to ~ 0.3 $mA.cm^{-2}$, where each stabilized. This increase was correlated to an increase in ΔC and Q_{1h}, confirming that mature EABs can be improved by applying more adequate periodic polarization [25]. Conversely, the transition in duty cycle from 67% to 50% did not significantly impact the electroactivity of $EAB_{67\%}$. We conjecture that the change in polarization parameters was too small to induce large changes in these already aged EABs. Finally, the two $EAB_{50\%}$ detached a second time at day 40, concomitant with a large decrease in current production from 1.0 $mA.cm^{-2}$ to 0.32 $mA.cm^{-2}$. These detachments were only partial and a fraction of the EABs stayed on the electrode surface (see detachment 2 in Figure 3). This time, only half of the previous maximum current was recovered (0.54 mA/cm^2), possibly because the incomplete removal of the EAB hindered the development of a fully fresh and active EAB. By the end of Phase II, the j_{ss} for all EABs were stabilized around 0.3 $mA.cm^{-2}$. Between this study and a previous one [25], we only observed spontaneous detachments for EABs periodically polarized with duty cycle of 50% and 10 s OCP-time. Those EABs were always the ones producing the highest current density, above 1 $mA.cm^{-2}$, which is substantially higher than the $\leq$ 0.5 $mA.cm^{-2}$ typical of continuously polarized acetate-fed EABs grown on flat surfaces at 28 °C [19]. It is impossible to conclude yet on the cause(s) leading to those detachments. Several non-exclusive causes could be proposed: (i) the high current density reached; (ii) the longer period fraction at which $EAB_{50\%}$ is under OCP i.e., at low electrode potentials (quickly stabilizing ~ − 0.45 V vs. Ag/AgCl [24]), indeed lower potentials have been shown to decrease the adhesion of single cells of *S. oneidensis* MR-1, a model electroactive bacterium [36], and adhesion of mammalian cells dramatically decreased when an underlying electrode was poised below its zero charge potential (i.e. with a negatively charged surface), at which point previously adhering cells could even detach [37]; (iii) periodic local pH variations at the electrode/EAB interface following the cycle of current spike (reconnection) and open circuit ─ though the medium was highly buffered; and (iv) a higher shear-stress imposed on $EAB_{50\%}$ which develop an uneven morphology (mushroom-like structure) while EABs grown under continuous polarization are flat, as shown in our previous study [24]. Importantly, the electrode surfaces in the present study were flat and smooth, and less detachment would be

expected for a rough surface or 3-dimensional porous electrodes due to better biofilm adhesion on rougher surfaces and/or physical retention within pores.

Phase III: artificial removal of aged EABs to improve performance

After 80 days of growth, the current production from all aged EABs (then all operated at 50% duty cycle) were considerably lower (~ 0.3 $mA.cm^{-2}$) than the initial maximum currents generated by fresh EABs under similar polarization (1.1 $mA.cm^{-2}$). Since aged-EABs appeared to specifically deliver lower current densities, we attempted to remove four EABs by performing hydrogen evolution at −15 $mA.cm^{-2}$ for 30 s. Biofilms were smoothly removed following this hydrogen gas bubble generation, low electrode potential and pH increase at the electrode/EAB interfaces. Such a removal is shown in Video S1. Periodic polarization with the previous duty cycle of 50% was immediately re-established for all EABs. The current j_{ss} initially decreased to zero for the 4 electrodes where EABs had been removed, before increasing again reaching pseudo-plateaus after 6 days to higher values (0.6 $mA.cm^{-2}$) than prior to EAB removal, or than controls who remained covered with aged-EABs (~ 0.35 $mA.cm^{-2}$). A similar pattern of recovery was observed for both the charge recovery parameters ΔC and Q_{1h}. However, none of the parameters describing the EAB performance could recover values as high as the ones reached by $EAB_{50\%}$ after the first growth, and the putative cause(s) for such behaviour is yet unclear.

Conclusions

We investigated the impact of different duty cycles on the electroactivity and charge recovery of EABs grown and delivering current under periodic polarization. Whereas studies performing short-term experiments typically advocate duty cycles between 75% and 95% to maximize performances, we observed that a smaller duty cycle (here 50%) induced the development of higher performing EABs, allowing substantially higher charge recovery even when considering the much longer OCP time intervals. The reason behind this discrepancy is very likely the longer timescale of the present experiment, allowing the specific polarization to modify the intrinsic characteristics of the EAB, probably following the overexpression of redox cofactors associated with the charge storage capacity and electron transport ability of the biofilm [24]. Such positive effects should however be tested at more relevant large-scale electrodes. Duty cycles below 50% may even generate more performant EABs over the long-term, but a trade-off with longer initial biofilm development would be expected.

We observed that EABs periodically polarized with a duty cycle of 50% detached twice over the course of the experiment. It is unclear if the detachment is due to the longer time of OCP (inducing highly reduced EAB even at the electrode surface and for longer time, periodically) and/or to the higher current spikes generated by these EABs.

We confirmed that EABs typically lose electroactivity while aging, possibly due to accumulation of less or non-active outer layers of biomass. We observed that these aged EABs can be quickly and easily removed from small, smooth carbon electrodes by applying a short but substantial H_2 evolution. The newly formed biofilms can at least partially recover their previous performance. This cathodic regeneration could also be tested on larger scale systems and with electrodes presenting a certain roughness or porosity, where biofilm removal would likely not be that straightforward.

The present findings provide valuable insight to grow EABs generating more charge over time or to replace aged EABs which have lost their previous optimal performances. This improvement enables MFCs to generate higher average power densities, or microbial electrochemical sensors exhibiting higher sensitivity. Though mostly overlooked until now, another putative outlook for periodic polarization of EABs resides in the fact that the nature of the polarization can, in some cases, highly impact the product distribution from microbial electrocatalysis. For example, Wang et al. showed that constantly polarized denitrifying microbial cathodes fully reduced nitrate to N2, while the periodically polarized cathodes reduced up to 30% of the consumed nitrate to nitrous oxide N_2O [38]. The incomplete denitrification was likely caused by the periodic deficit of electron supply induced by the OCP periods. While in that specific case the output was unfavorable because N_2O is a potent greenhouse gas, it appears relevant to assess the opportunity of optimizing the distribution of reaction products by tuning electrode polarization when metabolic intermediates are valuable chemicals.

Acknowledgements

X.Z. is financially supported by the China Scholarship Council (File no. 201406120043). A.P and K.R. are supported by the BOF19/GOA/026 (File no. 01G02619). A.P. is supported by FWO Research projects fundamental research G038520N. K.R., X.Z. are supported by FWO microelectronics G.0206.16N. A.L. is supported by ESA contract (4000113452/15/NL/AT).

References

1. Logan, B.E., *Exoelectrogenic bacteria that power microbial fuel cells.* Nature Reviews Microbiology, 2009. **7**(5): p. 375-381.
2. Rabaey, K. and R.A. Rozendal, *Microbial electrosynthesis — revisiting the electrical route for microbial production.* Nature Reviews Microbiology, 2010. **8**(10): p. 706-716.
3. Prévoteau, A. and K. Rabaey, *Electroactive Biofilms for Sensing: Reflections and Perspectives.* ACS Sensors, 2017. **2**(8): p. 1072-1085.
4. Guo, K., et al., *Flame Oxidation of Stainless Steel Felt Enhances Anodic Biofilm Formation and Current Output in Bioelectrochemical Systems.* Environmental Science & Technology, 2014. **48**(12): p. 7151-7156.
5. Guo, K., et al., *Engineering electrodes for microbial electrocatalysis.* Current Opinion in Biotechnology, 2015. **33**: p. 149-156.
6. Baudler, A., et al., *Does it have to be carbon? Metal anodes in microbial fuel cells and related bioelectrochemical systems.* Energy & Environmental Science, 2015. **8**(7): p. 2048-2055.
7. Pierra, M., et al., *Growth and current production of mixed culture anodic biofilms remain unaffected by sub-microscale surface roughness.* Bioelectrochemistry, 2018. **122**: p. 213-220.
8. Coursolle, D. and J.A. Gralnick, *Modularity of the Mtr respiratory pathway of Shewanella oneidensis strain MR-1.* Molecular Microbiology, 2010. **77**(4): p. 995-1008.
9. Reguera, G., et al., *Extracellular electron transfer via microbial nanowires.* Nature, 2005. **435**(7045): p. 1098-1101.
10. Glaven, S.M., *Bioelectrochemical systems and synthetic biology: more power, more products.* Microbial Biotechnology, 2019. **12**(5): p. 819-823.
11. Ieropoulos, I., et al., *Energy accumulation and improved performance in microbial fuel cells.* Journal of Power Sources, 2005. **145**(2): p. 253-256.
12. Grondin, F., M. Perrier, and B. Tartakovsky, *Microbial fuel cell operation with intermittent connection of the electrical load.* Journal of Power Sources, 2012. **208**: p. 18-23.
13. Walter, X.A., J. Greenman, and I.A. Ieropoulos, *Intermittent load implementation in microbial fuel cells improves power performance.* Bioresource Technology, 2014. **172**: p. 365-372.
14. Fradler, K.R., et al., *The effect of internal capacitance on power quality and energy efficiency in a tubular microbial fuel cell.* Process Biochemistry, 2014. **49**(6): p. 973-980.
15. Gardel, E.J., et al., *Duty Cycling Influences Current Generation in Multi-Anode Environmental Microbial Fuel Cells.* Environmental Science & Technology, 2012. **46**(9): p. 5222-5229.
16. Coronado, J., M. Perrier, and B. Tartakovsky, *Pulse-width modulated external resistance increases the microbial fuel cell power output.* Bioresource Technology, 2013. **147**: p. 65-70.

17. Liang, P., et al., *Performance enhancement of microbial fuel cell by applying transient-state regulation.* Applied Energy, 2017. **185**: p. 582-588.

18. Uría, N., et al., *Transient Storage of Electrical Charge in Biofilms of Shewanella oneidensis MR-1 Growing in a Microbial Fuel Cell.* Environmental Science & Technology, 2011. **45**(23): p. 10250-10256.

19. Bonanni, P.S., et al., *Charge accumulation and electron transfer kinetics in Geobacter sulfurreducens biofilms.* Energy & Environmental Science, 2012. **5**(3): p. 6188-6195.

20. Guo, F., J.T. Babauta, and H. Beyenal, *Impact of intermittent polarization on electrode-respiring Geobacter sulfurreducens biofilms.* Journal of Power Sources, 2018. **406**: p. 96-101.

21. Deeke, A., et al., *Capacitive Bioanodes Enable Renewable Energy Storage in Microbial Fuel Cells.* Environmental Science & Technology, 2012. **46**(6): p. 3554-3560.

22. Deeke, A., et al., *Influence of the thickness of the capacitive layer on the performance of bioanodes in Microbial Fuel Cells.* Journal of Power Sources, 2013. **243**: p. 611-616.

23. Borsje, C., et al., *Performance of single carbon granules as perspective for larger scale capacitive bioanodes.* Journal of Power Sources, 2016. **325**: p. 690-696.

24. Zhang, X., et al., *Periodic polarization of electroactive biofilms increases current density and charge carriers concentration while modifying biofilm structure.* Biosensors and Bioelectronics, 2018. **121**: p. 183-191.

25. Zhang, X., K. Rabaey, and A. Prévoteau, *Reversible Effects of Periodic Polarization on Anodic Electroactive Biofilms.* ChemElectroChem, 2019. **6**(6): p. 1921-1925.

26. Pereira, J., et al., *The effect of intermittent anode potential regimes on the morphology and extracellular matrix composition of electro-active bacteria.* Biofilm, 2021. **4**: p. 100064-100064.

27. Schrott, G.D., P.S. Bonanni, and J.P. Busalmen, *Open circuit potentiometry reports on internal redox states of cells in G. Sulfurreducens biofilms.* Electrochimica Acta, 2019. **303**: p. 176-182.

28. Dewan, A., H. Beyenal, and Z. Lewandowski, *Intermittent Energy Harvesting Improves the Performance of Microbial Fuel Cells.* Environmental Science & Technology, 2009. **43**(12): p. 4600-4605.

29. Zhang, X., et al., *Rapid and Quantitative Assessment of Redox Conduction Across Electroactive Biofilms by using Double Potential Step Chronoamperometry.* ChemElectroChem, 2017. **4**(5): p. 1026-1036.

30. Chadwick, G.L., et al., *NanoSIMS imaging reveals metabolic stratification within current-producing biofilms.* Proceedings of the National Academy of Sciences, 2019. **116**(41): p. 20716-20724.

31. Liu, Y. and D.R. Bond, *Long-distance electron transfer by G. sulfurreducens biofilms results in accumulation of reduced c-type cytochromes.* ChemSusChem, 2012. **5**(6): p. 1047-53.

32. Robuschi, L., J.P. Tomba, and J.P. Busalmen, *Proving Geobacter biofilm connectivity with confocal Raman microscopy.* Journal of Electroanalytical Chemistry, 2017. **793**: p. 99-103.

33. Robuschi, L., et al., *Spectroscopic Slicing to Reveal Internal Redox Gradients in Electricity‐Producing Biofilms.* Angewandte Chemie International Edition, 2013. **52**(3): p. 925-928.

34. Rossi, R., et al., *Continuous Flow Microbial Flow Cell with an Anion Exchange Membrane for Treating Low Conductivity and Poorly Buffered Wastewater.* ACS Sustainable Chemistry & Engineering, 2021. **9**(7): p. 2946-2954.

35. Reimers, C.E., et al., *Benthic microbial fuel cell systems for marine applications.* Journal of Power Sources, 2022. **522**: p. 231033.

36. Zhang, S., et al., *Deciphering Single-Bacterium Adhesion Behavior Modulated by Extracellular Electron Transfer.* Nano Letters, 2021. **21**(12): p. 5105-5115.

37. Guette-Marquet, S., et al., *The electrochemical potential is a key parameter for cell adhesion and proliferation on carbon surface.* Bioelectrochemistry, 2022. **144**: p. 108045.

38. Wang, X., A. Prévoteau, and K. Rabaey, *Impact of Periodic Polarization on Groundwater Denitrification in Bioelectrochemical Systems.* Environmental Science &